Journal of Molecular Liquids 413 (2024) 126012

Contents lists available at ScienceDirect

Journal of Molecular Liquids

journal homepage: www.elsevier.com/locate/molliq

Surface engineered novel cationic surfactants with enhanced surface adsorption for environmental applications

Seyid Zeynab Hashimzada [a,b], Vagif Abbasov [a], Rayen Ben Aoun [b,c], Narcisa Smječanin [b,d], Saida Ahmadbayova [a], Sabah Ansar [e], Farooq Sher [f,*]

[a] Institute of Petrochemical Processes, Ministry of Education of the Republic of Azerbaijan, Khojaly Avenue 30, Baku 1025, Azerbaijan
[b] International Society of Engineering Science and Technology, Nottingham, United Kingdom
[c] Faculty of Sciences of Tunis, University of Tunis El Manar, Tunis 1068, Tunisia
[d] Department of Chemistry, Faculty of Science, University of Sarajevo, Sarajevo 71000, Bosnia and Herzegovina
[e] Department of Clinical Laboratory Sciences, College of Applied Medical Sciences, King Saud University, P.O. Box 10219, Riyadh, 11433, Saudi Arabia
[f] Department of Engineering, School of Science and Technology, Nottingham Trent University, Nottingham NG11 8NS, United Kingdom

ARTICLE INFO

Keywords:
Gemini cationic surfactants
Molecular structure
Surface parameters
Conductivity analysis
DLS measurements
Antimicrobial activity

ABSTRACT

Gemini Cationic Surfactants (GCS) have garnered significant attention due to their distinctive molecular structure, featuring two hydrophilic head groups associated with a hydrophobic spacer. This distinctive configuration enables diverse applications across various fields. Hence, the current study introduces a novel series of GCSs, ethanediyl-1,2-bis[di(2-hydroxypropyl) alkylammonium] dibromide (C_n-C_2-C_n[IsoPr(OH)$_2$; n = 9, 12 and 14) and comprehensively explore their properties, highlighting their promising antimicrobial activity. The synthesis of GCSs was validated using ^{1}H NMR and IR spectroscopy. Dynamic Light Scattering was employed to determine the dimensions of Gemini surfactant aggregates in aqueous solutions. Surface tension analysis determined critical concentrations of micelle (CMC), minimum surface area (A_{min}) and concentration of surface excess (Γ_{max}). Physicochemical properties were assessed through conductivity and surface tension analyses in aqueous solutions. The CMC, A_{min} and Γ_{max} values decrease as alkyl chain length extends. Surface tension data revealed strong adsorption of GCSs at interfaces. π values (mN/m) ranged from 36.7 ($C_{14}C_2C_{14}$[Iso-Pr(OH)]$_2$) to 45.3 ($C_9C_2C_9$[Iso-Pr(OH)]$_2$). Conductivity and surface tension measurements further characterized Gemini surfactants in aqueous environments at 298 K. The size of the micelle aggregates varied between $C_9C_2C_9$[Iso-Pr(OH)]$_2$ (1.2885 nm) and $C_{14}C_2C_{14}$[Iso-Pr(OH)]$_2$ (1.9210 nm), highlighting the impact of chain length on micelle size. Hence, the study highlights significant effect of the chain lengths on Gemini cationic surfactants' self-assembly in dilute aqueous environments. Antimicrobial tests demonstrated significant activity of C_n-C_2-C_n[IsoPr(OH)]$_2$ GCSs at varying concentrations. Antimicrobial tests showed the significant antimicrobial potential of these GCS compounds, suggesting their potential and promising applications in medical, hygiene, environmental sanitation and advanced materials sectors.

1. Introduction

Recently, there has been a surge of interest and investigation in the field of surfactant chemistry, particularly regarding a novel class of compounds called Gemini cationic surfactants (GCS) [1]. Their unique molecular architecture, characterized by two hydrophilic head groups linked by a hydrophobic chain has fascinated researchers and inspired extensive studies into their properties and potential applications. These surfactants exhibit enhanced physical and chemical characteristics [2], decreased critical concentration of micelle (CMC), improved solubility, foaming and moistening characteristics [3]. The symmetrical structure of GCSs, where hydrophobic and hydrophilic segments share similar configurations, plays a crucial role in micelle formation. Dimeric Gemini surfactants, distinguished by their lower CMC values require fewer molecules than their monomeric counterparts for micelle formation [4].

Gemini surfactants (GS) physicochemical properties are primarily determined by their molecular configurations, e.g., the charge of hydrophilic portions, hydrophobic chain lengths and spacer length and nature. Cationic Gemini surfactants (CGS) are alkyl ammonium species with two long hydrophobic chains linked by nitrogen atoms and a spacer

* Corresponding author at: Department of Engineering, School of Science and Technology, Nottingham Trent University, Nottingham NG11 8NS, UK.
E-mail address: Farooq.Sher@ntu.ac.uk (F. Sher).

https://doi.org/10.1016/j.molliq.2024.126012
Received 14 March 2024; Received in revised form 9 September 2024; Accepted 12 September 2024
Available online 15 September 2024

chain which has proven essential in surfactant formation [5]. Distinctive from other surfactant types, alkyl ammonium-type surfactants exhibit exceptional surface activity and potent antimicrobial properties as demonstrated in the study of Moosavi et al. [6]. The outstanding properties of Gemini surfactants are expanding their field of application over the years emerging in a variety of sectors, including hard surface cleaning, food processing and therapeutic applications [7]. Lately, a rising number of investigations have arisen regarding the exploration and investigation of cationic surfactants containing hydroxyl groups [8]. The hydroxyl group's presence significantly impacts their critical micelle concentration, enhancing their potential effectiveness [9].

In Gemini ammonium-type cationic surfactant, the appearance of hydroxyl groups in both the spacer and functional group attached to nitrogen atom significantly influences adsorption and micelle formation properties. The aromatic or aliphatic group, shorter $(CH_2)_2$ or longer $(CH_2)_{6\text{-}12}$ methylene group, polar polyether group and rigid (stilbene, benzene or elastic polyethene) groups are used to control the division between the main groups [10]. In the domain of GCSs, various studies have highlighted the influence of structural modifications on activity and surface properties. As an antimicrobial property, the main feature of cationic surfactants is their electrostatic and hydrophobic effect on cell membranes [11]. Recent research efforts have focused on optimizing the efficacy of these surfactants at lower doses, yielding promising results. Additionally, it is noteworthy that certain conventional quaternary ammonium surfactants could also exhibit harmful side effects [12] by affecting cell biomembranes [13].

Currently, extensive research is being done to synthesize antimicrobial surfactants with fewer adverse effects. In surfactants, alkyl chain lengthening is linked to a reduction in CMC values and an improvement in antimicrobial activity. For this reason, numerous references indicate that antimicrobial properties are contingent on both the critical concentration of micelle value and the length of the alkyl chain. Thus, antimicrobial quality improves with decreasing CMC value. The adsorption of surfactants onto cell membranes increases while alkyl chain elongates [14]. Xu et al. [15] revealed the increased surface activity of Gemini CS compared to their monomeric counterparts, as well as the impact of the length of alkyl chains C_{12}, C_{14} and C_{16} on their properties. They studied aggregation ability and surface activity properties by various physicochemical methods. Further studies by Hussain et al. [16] synthesized amidoamine-type GCSs with rigid and flexible spacer groups, revealing that the *trans*-conformation GCS exhibited enhanced surface activity. Both spacer length and structure were highlighted as playing a role, with the flexible hydrophilic spacer contributing to efficient micelle formation [16].

Molecular-scale structural optimization appears to be crucial, as emphasized by Zhou et al. [17]. The ability to modify hydrophobic and hydrophilic head groups [18], along with spacer characteristics, offers an exciting opportunity to enhance surfactant performance [19]. Similarly, Taleb et al. [20] highlighted a systematic approach to synthesizing efficient cationic Gemini surfactants, which is based upon the reaction of quaternization for N,N,N′,N′-tetramethylalkylenediamine 2-bromo-N-(4-(alkyloxy) phenyl) acetamide species and retains a benzene ring held by the side chain. They investigated the interaction between the dimensions of the group spacers and the chain of alkyls, evaluating both colloidal and chemical variations as well as antimicrobial properties. Specifically, the spacer and hydrophobic chain were identified as key factors influencing aggregation performance [20]. The synthesis of Gemini CSs with hydroxyl groups in the head group has attracted more attention from researchers. These Gemini CSs, characterized by hydroxyl groups in their hydrophilic fragment, exhibit unique properties compared to GCSs featuring other small alkyl groups (methyl, ethyl, and propyl etc.).

Nevertheless, current research in this field faces significant limitations, including limited comprehension of the effects of isopropylol groups, the necessity of comprehensive comparative analyses of structural components, limited exploration of micelle aggregation kinetics and insufficient insight into the mechanisms driving antimicrobial potential. This study addresses these gaps by employing advanced techniques such as ^{1}H NMR and FTIR spectroscopy to validate the chemical structure of these novel Gemini cationic surfactants (GCSs). Hence, this study conducted a thorough comparative analysis, highlighting the influence of isopropyl groups on crucial parameters, like critical concentration of micelle, minimum surface area (A_{min}) and excess surface concentration (Γ_{max}). Furthermore, the mechanisms behind the promising antimicrobial potential of these Gemini CSs are elucidated by in-depth antimicrobial testing at different concentration ranges (8, 4 and 2 mg/mL). In tandem, the aggregate size distribution established in aqueous systems of the synthesized Gemini surfactants utilizing Dynamic Light Scattering (DLS) was also assessed, offering a comprehensive view of their behaviour. Current research foreshadows Gemini's potential application in eco-friendly and efficient drug delivery systems, thereby enhancing the precision and effectiveness of pharmaceutical delivery.

Table 1
Equations employed for determination of surface tension and electrical conductivity analysis.

Equation name	Equation	Equation number	Reference
Equivalent apparent hydrodynamic diameter	$Dh = kT\tilde{A}\cdot 3\pi\eta D$	(1)	[20]
Gibbs free energy of micellization	$\Delta G_m^{\circ} = RT(1+2\beta)lnX_{CMC}$	(2)	[59]
Standard Gibbs free energy of adsorption	$\Delta G_{ad}^{\circ} = \Delta G_m^{\circ} - \pi_{CMC}\tilde{A}\cdot\Gamma_{max}$	(3)	[26]
Maximum surface excess concentration	$\Gamma_{max} = \frac{-1}{nRT}\times(\frac{d\gamma}{dlnC})_T$	(4)	[27]
Minimal area per surfactant molecule	$A_{min} = 10^{16}\times(N_A\Gamma_{max})^{-1}$	(5)	[28]
Surface tension reduction	$\pi_{CMC} = \gamma_0 - \gamma_{CMC}$	(6)	[29]
Critical packing parameters	$P = \frac{V}{a_{0\times l_c}}$	(7)	[60]
Volume of hydrophobic chain	$V = (0.0274+0.0269n_n)nm^3$	(8)	[60]
Critical length of hydrophobic chain	$l_0 = (0.0274+0.1265n)nm$	(9)	[61]

2. Experimental procedures and materials

"Organic Synthesis" plant provided propylene oxide (99.97–99.98%) (Sumgait, Azerbaijan). Ethylenediamine (UK), 1-bromononane (Germany) and 1-bromododecane (UK) were from Alfa Aesar and 1-bromotetradecane (Japan) was provided by Sigma-Aldrich. Structural characterization tools, including NMR and FTIR spectroscopy, were utilized to support the molecular composition of all synthesized Gemini surfactants (GS). FTIR data was collected using KBr disks on ALPHA FT-IR spectrometer (Bruker) [21]. ^{1}H NMR spectra were acquired utilizing a Bruker TOP SPIN spectrometer operating at selected frequencies. Chemical shifts (δ scale was in ppm) were referenced to TMS and CDCl3 was utilized as solvent [22]. To analyse the distribution of aggregate dimensions formed in water-based systems of the prepared Gemini surfactants, Dynamic Light Scattering (DLS) analysis was performed at 298.15 K utilizing an analyser for particle size (HORIBA LB-550, Japan). With a650 nm laser diode emitting light at a power of 5 mW was used for illumination. The size measurement range encompassed dimensions from 1 nm to 6 μm [23]. Sample concentrations of 0.1, 0.2 and 0.3% were utilized, with each sample subjected to a minimum of three measurements. The diffusion coefficient distribution (D) of the solutes was determined through the analysis of diffusion data using the CONTIN technique applied to the correlation function [24]. Furthermore, the equivalent apparent hydrodynamic diameter (Dh) is evaluated by the Stokes-Einstein equation in Table 1 (Eq. (1)), where k is the constant of

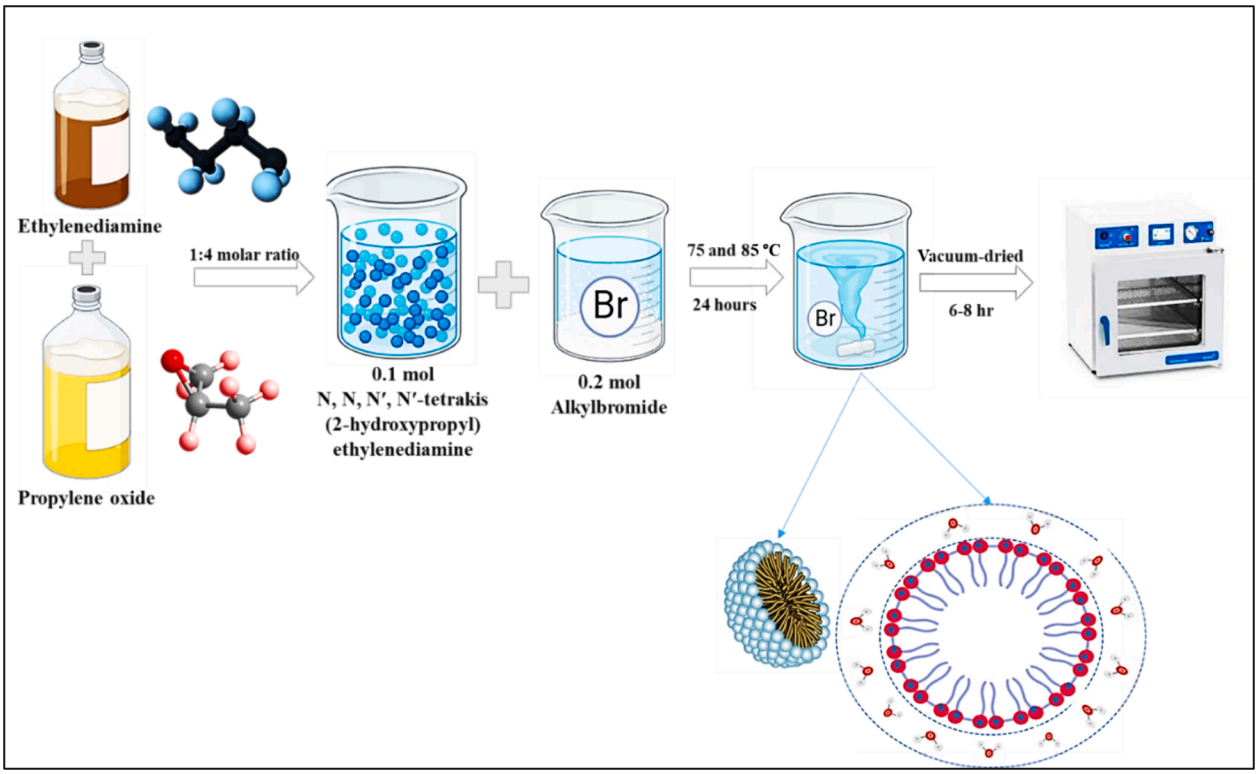

Fig. 1. Experimental setup from the current study of Gemini cationic surfactant synthesis.

Boltzmann, T is the absolute temperature and η is the coefficient of viscosity for solvent [20].

2.1. Preparation method for Gemini cationic surfactants

The product was synthesized in two stages outlined in Fig. 1. Firstly, N,N,N′,N′-tetrakis(2-hydroxypropyl) ethylenediamine was produced by reacting ethylenediamine and propylene oxide reacted at a 1:4 M ratio [24]. Structural confirmation of obtained N,N,N′,N′-tetrakis(2-hydroxypropyl) ethylenediamine was conducted using NMR and IR spectroscopy methods. Subsequently, symmetric CGS synthesis involved combining 0.1 mol of product from the first step with 0.2 mol of alkyl bromide (n = 9, 12, and 14). The mixture was continuously agitated at a temperature of between 75 and 85 °C using a magnetic stirrer and a

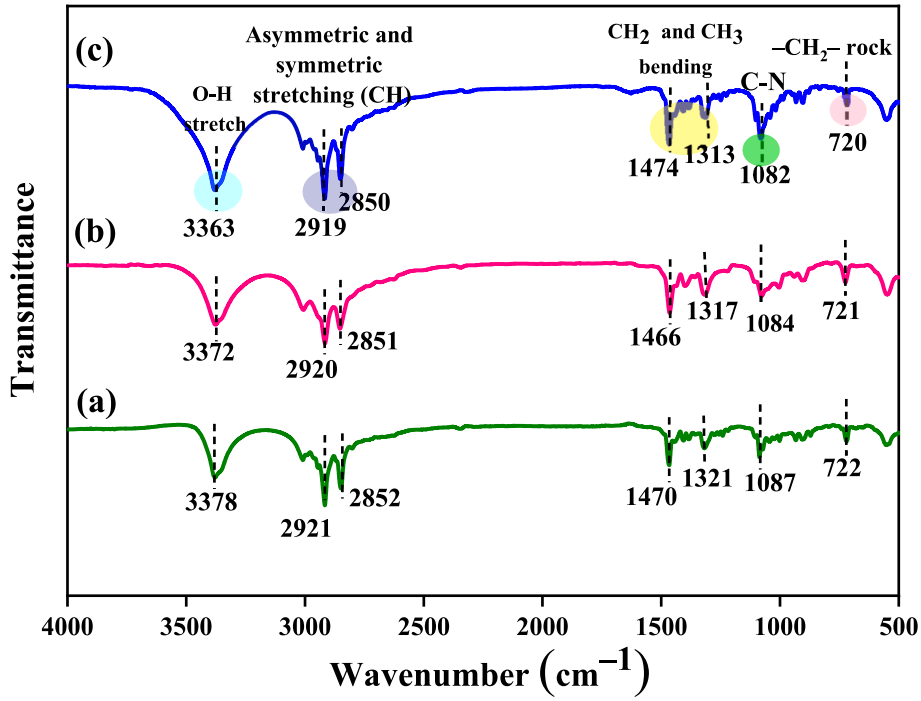

Fig. 2. FTIR spectras; (a) $C_9C_2C_9$[Iso-Pr(OH)]$_2$, (b) $C_{12}C_2C_{12}$[Iso-Pr(OH)]$_2$ and (c) $C_{14}C_2C_{14}$[Iso-Pr(OH)]$_2$ for obtained Gemini surfactants.

heating device for 24 h [20]. Following rinsing with hexane, the material was subjected to four to five cycles of recrystallization using an acetone/ethanol solvent and was then vacuum-dried for 6–8 hr, yielding the product with an estimated 93% reaction efficiency. The efficiency of the reaction was approximately 93%. The obtained compounds exhibited a purity level of 95–97%. Obtained from N,N,N′,N′-tetrakis (2-hydroxypropyl) ethylenediamine and tetradecyl bromide, $C_nC_2C_n$[*iso*-Pr(OH)]$_2$ is freely soluble in organic solvents like acetone, ethanol, ethyl acetate and water, slightly soluble.

2.2. Surface tension and electrical conductivities analysis

For the solutions of surfactants, the air–water interfaces and their tensions of surface were studied via a KSV Sigma 702 tensiometer (Finland) with a du Nouy ring and the ring detachment method. Before measuring, the samples were mixed with the double distilled water and the tension of surface at the perimeter of the double distilled water and the air was validated to be 72 mN/m. Three measurements were performed for each sample. The analyses were conducted at 298 K considering a temperature difference of 0.01 K. All the measurements were precise to within ±0.2 mN/m. The micellization Gibbs free energy for dimeric surfactants, ΔG^0_m, was derived from the molar fraction at the micelle critical concentration, X_{CMC} and the extent of dissociation for counterion (Eq. (2)) in Table 1. Here, R is the gas constant, universal (8.314 J/mol K); β denotes the degree of binding for counterions; X_{CMC} is the CMC in mole fraction (X_{CMC}=CMC/55.4), with units mol/L [25]. The constant 55.4 is calculated from 1 L to 55.4 mol equivalency of water at 298 K.

Since thermodynamically stable micelles form spontaneously, energy values without micellization are negative. The adsorption ΔG^0 was determined by the equation shown below (Eq. (3)) [26]. The concentration maximum surface excess at CMC (Γ_{max}) was derived from the equation given for Gibbs energy (Eq. (4)). Where γ refers to the tension of surface at CMC and C is the surfactant used concentration in an aqueous system [27]. The factor dγ/dlogC was derived from the slopes of the linear graphs of γ versus logC immediately before the CMC (Fig. 2) in Table 1. The γ-log concentration diagrams offer information about the surface occupancy per molecule at the interface of air water as well as efficiency of the used surfactant. The minimal area per molecule of surfactant (A_{min}) at the air–solvent boundary was derived from equation (Eq. (5)). Where N_A is the constant of Avogadro [28]. The efficiency of reduction for CMC surface tension (Π_{CMC}), one of the surface parameters, is employed to assess the effectiveness of $C_nC_2C_n$[*iso*-Pr(OH)]$_2$ surfactants in reducing water surface tension.

In general, a higher value of π_{CMC} indicates greater effectiveness of the surfactant. The determined Π_{CMC} is calculated as given in Eq. (6). Where γ_0 and γ_{CMC} denote the surface tensions of double distilled water and Cn-s-Cn cationic surfactants aqueous solution at CMC, respectively [29]. The critical packing parameters (CPP or P) of the produced Gemini surfactants were calculated (Table 1) (Eq. (7)). Here, a_0 is the sectional area of the group which has hydrophilic head of the molecule of surfactant (nm), V is the volume of the hydrophobic chain (nm^3) and l_0 is the critical length of the hydrophobic chain (nm) (≤max it can be stretched) [30]. When analysing the Gemini surfactants in question, $a_0 = A_{min}$, V and l_0 were calculated using the Eqs. (8) and (9). Here, n is the carbon atom number in the micelle alkyl [31]. Various Gemini surfactant concentration solutions in the range from 0.001 to 2% were prepared and their specific electrical conductivities (κ) were recorded by an "ANION 4120" conductometer at 298 K. The measurements were repeated three times. Double distilled water, with a specific electrical conductivity varying from 1.2 to 1.5 μS/cm at the indicated temperature (temperature fluctuation: ±0.1 K), was utilized to prepare the aqueous solutions. Uncertainty of measurement turned out to be a relative error of no more than ±2%.

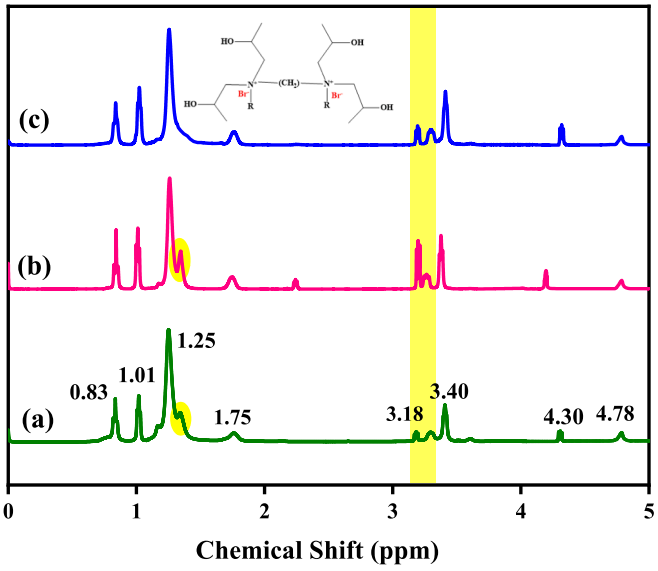

Fig. 3. ^{1}H NMR spectrum; (a) $C_9C_2C_9$[Iso-Pr(OH)]$_2$, (b) $C_{12}C_2C_{12}$[Iso-Pr(OH)]$_2$ and (c) $C_{14}C_2C_{14}$[Iso-Pr(OH)]$_2$ for obtained Gemini surfactants.

2.3. Antibacterial and antifungal activity analysis

The antimicrobial characteristics of the surfactants were evaluated utilizing the disk diffusion method. Laboratory strains were obtained using thick (*Staphylococcus aureus*, *Pseudomonas aeruginosa*) and thin cell-walled (*Escherichia coli*) bacteria and the fungi *Candida albicans*. Bacteria with varying cell wall thicknesses were grown on Sabouraud medium, while the fungus mentioned was grown on peptone agar. Microbial suspensions were prepared with a concentration of 1 billion cells per millilitre, following the method of disk diffusion each suspension was applied to the surface of corresponding nutritive medium using buffers. Sterile paper disks, 6 mm in diameter, were soaked with three different concentrations (8, 4, and 2 mg/mL) of each CGA and placed on cultured medium containing bacteria and fungi [32]. The plates were kept at 37 °C for 24 h. The antimicrobial activity was investigated by evaluating the diameter of zone of inhibition (in mm). This procedure was repeated three times, utilizing sterile water as a negative probe.

3. Results and discussion

3.1. Spectral characteristics of prepared surfactants

FTIR spectra of the prepared compounds showed absorption bands given in Fig. 2. The band with very strong intensity at 3378 cm^{-1} is attributed to O—H group vibrations. The peaks at 2855 cm^{-1} and 2921 cm^{-1} could correspond to the asymmetric and symmetric vibrations of the CH_2 groups. The band at 1088 cm^{-1} corresponds to the stretching vibration of C—N$^+$ bond, while the band at 722 cm^{-1} assigns to the rocking vibration of CH₂ groups. The FTIR spectra confirmed the existence of the desired functional groups. Similarly, $C_{12}C_2C_{12}$[Iso-Pr(OH)]$_2$ show very strong intensity at 3372 cm^{-1} is assigned to the O—H group vibrations. The peaks at 2851 cm^{-1} and 2920 cm^{-1} could be assigned to the symmetric and asymmetric vibration of CH_2 groups. The bands at 1474 cm^{-1} and 1313 cm^{-1} are a result of CH_2 and CH_3 bending vibrations, respectively. At 1084 cm^{-1}, the band corresponds to the stretching vibration of C—N$^+$ bond and for 721 cm^{-1}, corresponds to the rocking vibration of CH₂ groups. This reveal is in accordance with the study of Hussain et al. [21], who studied three cationic poly(ethylene oxide) Gemini surfactants (GSs) containing rigid and flexible spacers. Finally, the FTIR spectra of $C_{14}C_2C_{14}$[Iso-Pr(OH)]$_2$ show the following absorption bands at 720 cm^{-1} (CH_2 rocking), 1082 cm^{-1} (C—N$^+$), 2919 and

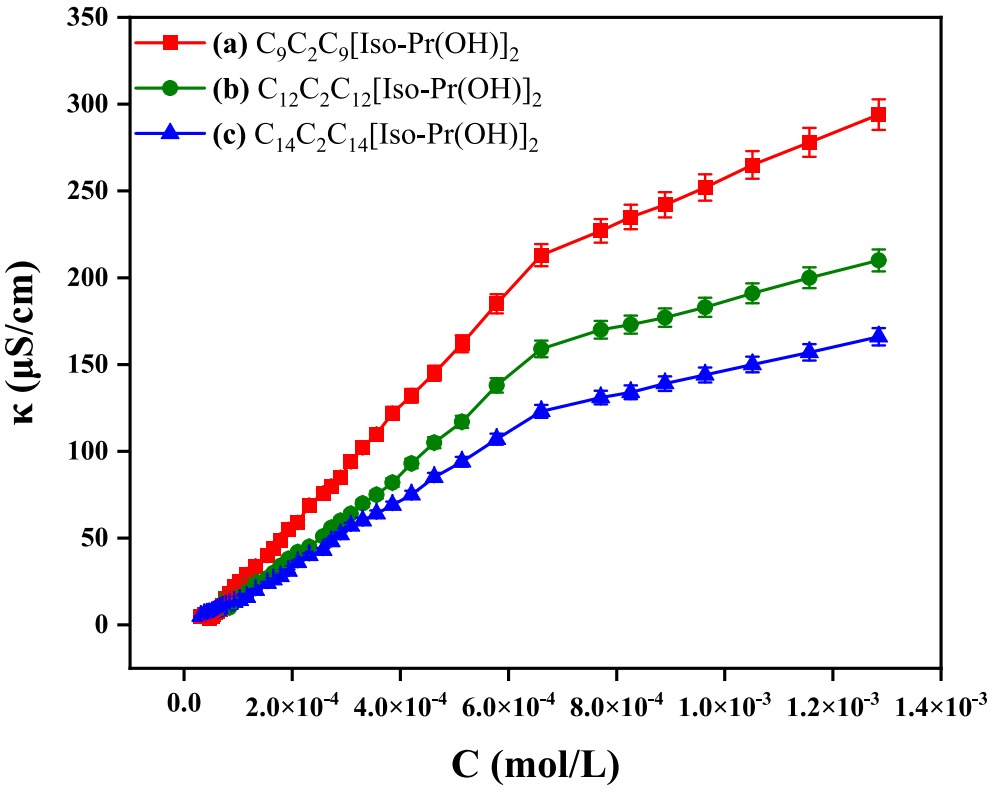

Fig. 4. Conductometric isotherms; (a) $C_9C_2C_9$[Iso-Pr(OH)]$_2$, (b) $C_{12}C_2C_{12}$[Iso-Pr(OH)]$_2$ and (c) $C_{14}C_2C_{14}$[Iso-Pr(OH)]$_2$ for obtained Gemini surfactants.

2850 cm^{-1} (C—H in —CH_3 or —CH_2—), 3363 cm^{-1} (—OH) corroborating the presence of the intended groups in each of prepared compound.

In agreement with our findings, Vasileva et al. [33] reported similar trends in a novel homologous series of Gemini dicationic surfactants (where n = 10, 12, 14). The ^{1}H NMR spectra of representative cationic Gemini surfactants (300 MHz, DMSO-d_6, δ/ppm) are shown in Fig. 3. For $C_9C_2C_9$[Iso-Pr(OH)]$_2$, the NMR spectrum reveals distinct peaks, with chemical shifts at 0.84 (triplet, 6H, a-H), 1.01 (doublet, 12H, b-H), 1.26 (multiplet, 40H, c-H), 1.74 (multiplet, 8H, d-H), 3.19 (triplet, 8H, e-H), 3.76 (doublet, 8H, f-H) and 4.19 (multiplet, 8H, g-H). These peaks provide insights into the structural features of $C_9C_2C_9$[Iso-Pr(OH)]$_2$. For $C_{12}C_2C1_2$[Iso-Pr(OH)]$_2$, NMR spectrum exhibits peaks similar to $C_9C_2C_9$ [Iso-Pr(OH)]$_2$, with chemical shifts at 0.84 (triplet, 6H, a-H), 1.01 (doublet, 12H, b-H), 1.26 (multiplet, 40H, c-H), 1.74 (multiplet, 8H, d-H), 3.19 (triplet, 8H, e-H), 3.76 (doublet, 8H, f-H) and 4.19 (multiplet, 8H, g-H).

The prominent peak at 2.24 ppm in ^{1}H NMR spectrum of substance $C_{12}C_2C_{12}$[Iso-Pr(OH)]$_2$ likely corresponds to the protons in isopropyl groups. This is because protons in alkyl chains typically resonate around 0.8 to 2.0 ppm in ^{1}H NMR spectrum and isopropyl groups would contribute to this region due to their alkyl nature [34]. The specific chemical environment of these protons, likely influenced by the neighbouring carbon atoms and any adjacent functional groups, could cause slight variations in their chemical shift. For $C_{14}C_2C_{14}$[Iso-Pr(OH)]$_2$, its NMR spectrum displays peaks with chemical shifts at 0.83 (triplet, 6H, a-H), 1.02 (doublet, 12H, b-H), 1.25 (multiplet, 40H, c-H), 1.76 (multiplet, 8H, d-H), 3.19 (triplet, 8H, e-H), 3.41 (doublet, 8H, f-H), and 4.31 (multiplet, 8H, g-H). These NMR shifts reflect the unique structural attributes of $C1_4C_2C_{14}$[Iso-Pr(OH)]$_2$. This analysis is consistent with the study of Parikh et al. [35] for a cationic GS series with differing alkyl chain lengths (n = 12 and 14).

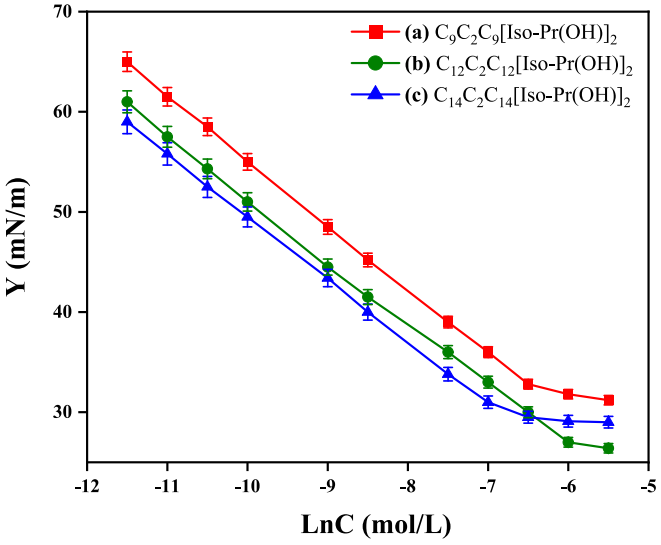

Fig. 5. Surface tension versus natural logarithmic concentration plot; (a) $C_9C_2C_9$[Iso-Pr(OH)]$_2$ (b) $C_{12}C_2C_{12}$[Iso-Pr(OH)]$_2$ and (c) $C_{14}C_2C_{14}$[Iso-Pr(OH)]$_2$ for obtained Gemini surfactants.

3.2. Surface activity analysis

Surface tension results are utilized to determine surface activity of CGS solutions. The surface activity of CGS mixtures was evaluated across a series of different concentrations at values below and above CMC as shown in Figs. 4 and 5. Values of various surface properties (ΔG^0_m, ΔG^0_{ad}, A_{min}, Γ_{max} and π_{CMC} are highlighted in Table 2. The surface tension of aqueous CGS solutions exhibited a linear decrease as the increase in concentration was observed. This trend leads to the identification of two distinct stages within the surfactant solution. It's important to

Table 2
Gemini surfactants properties overview regarding Gibbs free energy, packaging and surface activity.

Gemini surfactants	β	$\Gamma_{max} \times 10^{10}$ (mol/cm^2)	A_{min} (Å^2)	γ_{CMC} (mN/m)	π (mN/m)	l_0 (nm)	V (nm^3)	A_{min} (nm)	P	ΔG_{mic} (kJ/mol)	ΔG_{ad}
$C_9C_2C_9$[Iso-Pr(OH)]$_2$	0.45	0.89 ± 0.02	191.1	26.7 ± 0.5	45.3 ± 0.5	1.2885	0.2695	1.504	0.31	−29.18 ± 0.02	−35.42 ± 0.01
$C_{12}C_2C_{12}$[Iso-Pr(OH)]$_2$	0.42	0.85 ± 0.01	194.6	33.1 ± 0.3	38.9 ± 0.3	1.6680	0.3502	1.203	0.35	−27.52 ± 0.01	−32.08 ± 0.01
$C_{14}C_2C_{14}$[Iso-Pr(OH)]$_2$	0.38	0.84 ± 0.02	197.4	35.3 ± 0.3	36.7 ± 0.3	1.9210	0.4040	0.877	0.48	−26.44 ± 0.04	−30.80 ± 0.04

emphasize that measurement of surface tension is a classic method for investigating and evaluating the critical micelle concentration of surfactants. CMC values could be easily identified by observing the breaking point in surface tension instead of relying solely on concentration curves. According to a study by Hao et al. [36], the critical concentration of micelle (CMC), and the surface tension of the tested solution gives a rapid decrease with increasing concentration of surfactant. In addition, Betiha et al. [37] demonstrated that as the alkyl chain length increased, the surface activity of the compounds exhibited a gradual and noteworthy improvement, underscoring the effect of alkyl chain length on the effectiveness of reducing surface tension. Wang et al. [38] observed a clear correlation between surfactant concentration and surface tension, where higher surfactant concentrations led to reduced surface tension, possibly attributed to molecular entanglement [38].

A variety of surface tension (γ) at 298 K as a dependent on concentration is given in Fig. 5. The obtained CMC values, along with other parameters for surface activity are listed in Table 2. The results indicate that Gemini surfactants carry longer hydrophobic chains which increase the minimum surface tension of CnC2Cn[*iso*-Pr(OH)]$_2$ and have a diminished CMC value of surfactant. Increased hydrophobic interaction among longer alkyl chains, C_9–C_{14}, gradually decreases CMC value. This trend is consistent with conventional surfactants, as shown in the research of Sarikaya et al. [39]. Conversely, the surface tension value of the synthesized surfactants ranged between 26.5 and 31.5 mN/m, whereas in the case of alkyl chain lengths (n) equal to 8, 10 and 12, as synthesized by Ren et al. [40] this parameter was notably higher with the value of 35–39 mN/m. Diverse perspectives among researchers have led to varying viewpoints regarding the fluctuations in the price of A_{min}. Some studies suggest that an increase in the value of A_{min} is influenced by the larger size of GCS molecule. Conversely, other researchers propose that this effect is associated with the more compact packing of GCS molecules [41]. In the context of this investigation, it was observed that the value of A_{min} exhibited an upward trend as the length of alkyl chain increased from C_9 to C_{14}. This phenomenon highlights the effect of alkyl chain length on the price of A_{min}. Higher π_{CMC} values correspond to improved GCS properties. Among the surfactants studied, GCS with a C_9 alkyl chain has a remarkably higher π_{CMC} value. Therefore, GCS with alkyl chain length 9 is more efficient than other surfactants, showing a

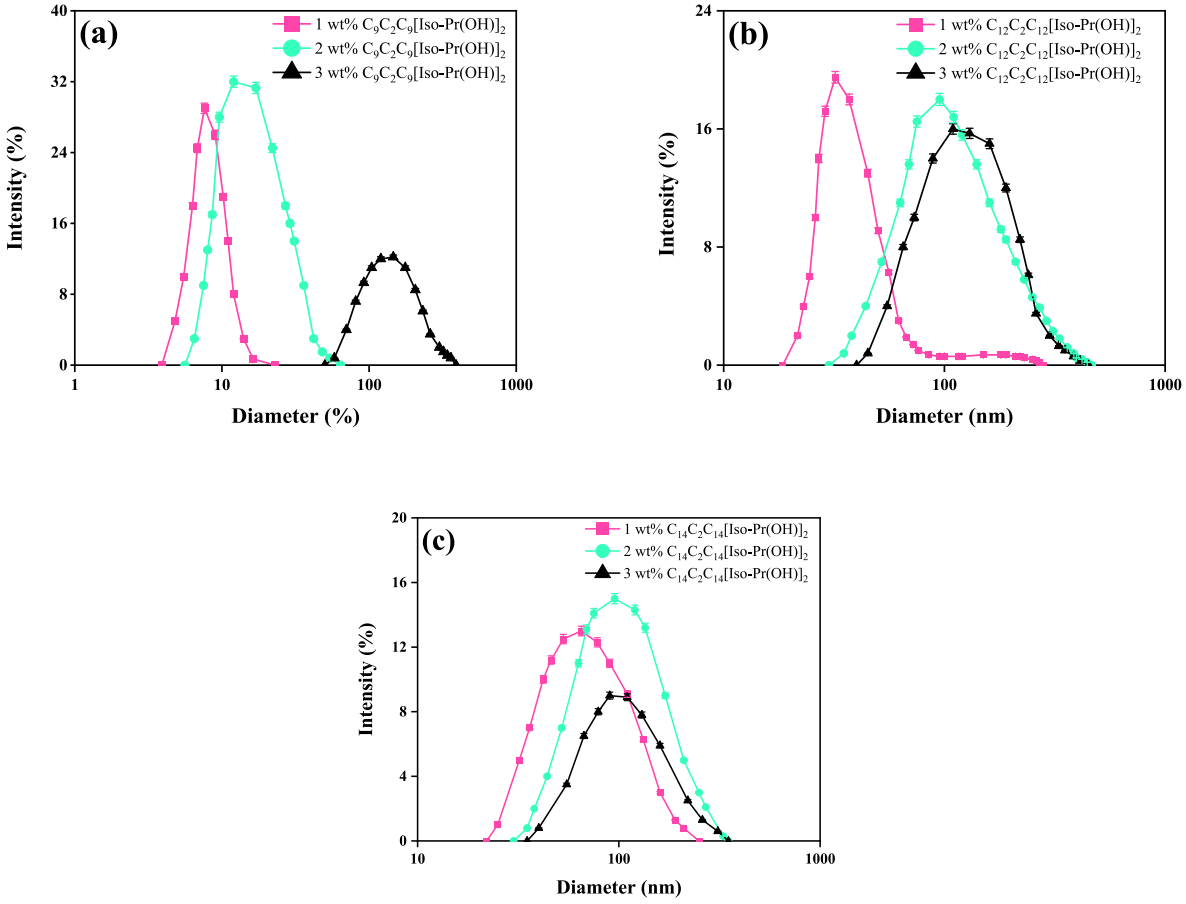

Fig. 6. DLS measurements of the size distributions; (a) $C_9C_2C_9$[Iso-Pr(OH)]$_2$, (b) $C_{12}C_2C_{12}$[Iso-Pr(OH)]$_2$ and (c) $C_{14}C_2C_{14}$[Iso-Pr(OH)]$_2$ at different concentrations 1, 2 and 3 wt%.

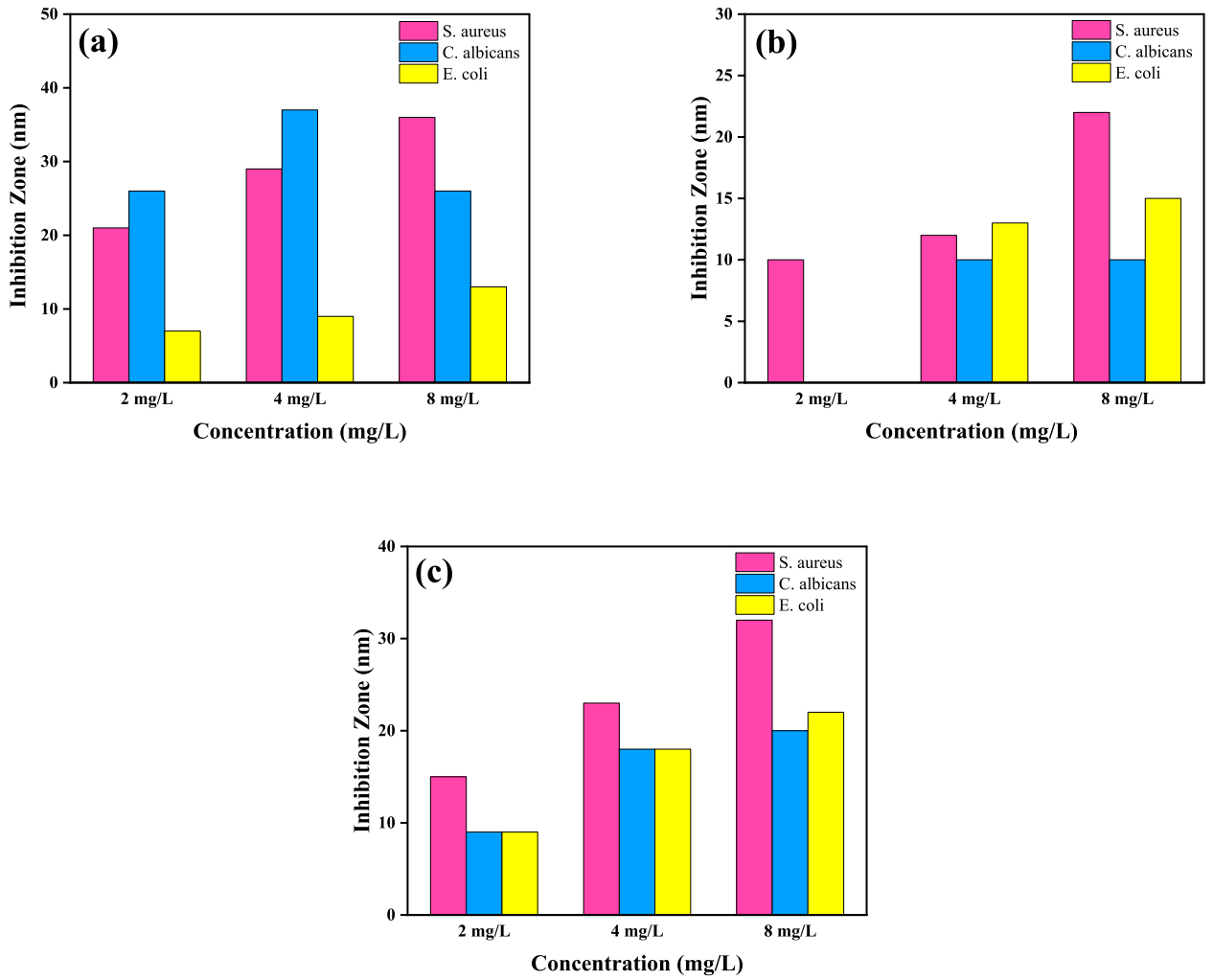

Fig. 7. The effects of antimicrobial activities; (a) $C_9C_2C_9$[Iso-Pr(OH)]$_2$, (b) $C_{12}C_2C_{12}$[Iso-Pr(OH)]$_2$ and (c) $C_{14}C_2C_{14}$[Iso-Pr(OH)]$_2$ at three different concentrations.

lower surface tension value than GCS with lengths of alkyl chain C_{12} and C_{14} [42].

Extending the alkyl chain length in the hydrophobic segment of both Gemini surfactant groups consistently influenced several key parameters. These included critical packing concentration (CPC), critical concentration of micelle (CMC), maximum excess surface concentration (Γ_{max}), beta (β), Gibbs free energy of micellization and adsorption (ΔG_{mic} and ΔG_{ad}), minimum surface area (A_{min}) and pC20 values. The nature of alkyl chain length and spacer notably affected the micellar microenvironment, highlighting the significant relationship between alkyl chain length and the properties of Gemini surfactants [35]. As shown in Table 2, surfactants' P values are in the range $1/3 < P < 1/2$, indicating that they form cylindrical micelles in aqueous solutions [43]. The data in Table 2 reveals that the counterion coupling degree of GS diminishes as the alkyl chain lengthens. Consequently, longer alkyl chains and an increased number of isopropyl groups in the hydrophilic part inhibit the recombination of dissociated counterions with the ammonium group.

Therefore, in these cases the value of α increases while that of β decreases. The values of Γ_{max} and π_{CMC} exhibit an inverse relationship to the length of the alkyl chain and the isopropyl group number in the hydrophilic portion. The Gibbs free energy changes of the micellization and adsorption procedures of the synthesized surfactants decrease with chain lengthening and increase with a growing number of isopropyl groups. Singh et al. [44] suggest that the micellar interaction parameter (β_m) is influenced by the spacer type in cationic Gemini surfactants, showing stronger attractive interactions with 16-Isb-16 as the spacer. This aligns with prior research indicating that shorter spacer chains result in reduced β_m in cationic Gemini mixtures, underlining the complex link between spacer chain length and β_m [44].

3.3. Specific electrical conductivity

Initially, the conductivity increases linearly as a function of the surfactants' concentration. Subsequently, an intersection with another linear dependence appears. The intersection points of these two lines agree to the critical micelle concentration, as illustrated in Fig. 4 and Table 2. This indicates the activity of GCS molecules and as a result, the formation of a micelle, which is accompanied by an increase in their permeability. The conductivity curves provide insight into several parameters, including the critical micelle concentration, Gibbs free energy of micellization and the degree of ionization. Recent studies have increasingly focused on hydroxyl group-containing GCSs. Their critical micelle formation density is extremely low because the value of CMC in GCSs is smaller when the hydrophilic part has a hydroxyl group as stated in the study of Zhao et al. [45]. In GCSs of the ammonium type, the hydroxyl group can be present both in the spacer and in the functional group attached to the nitrogen atom. The adsorption and micelle formation properties of GCSs are primarily influenced by their molecular structure [46]. Therefore, GCSs can be precisely tailored at the molecular level through structural modifications. This customization could be achieved by altering the hydrophobic alkyl chains [47], hydrophilic

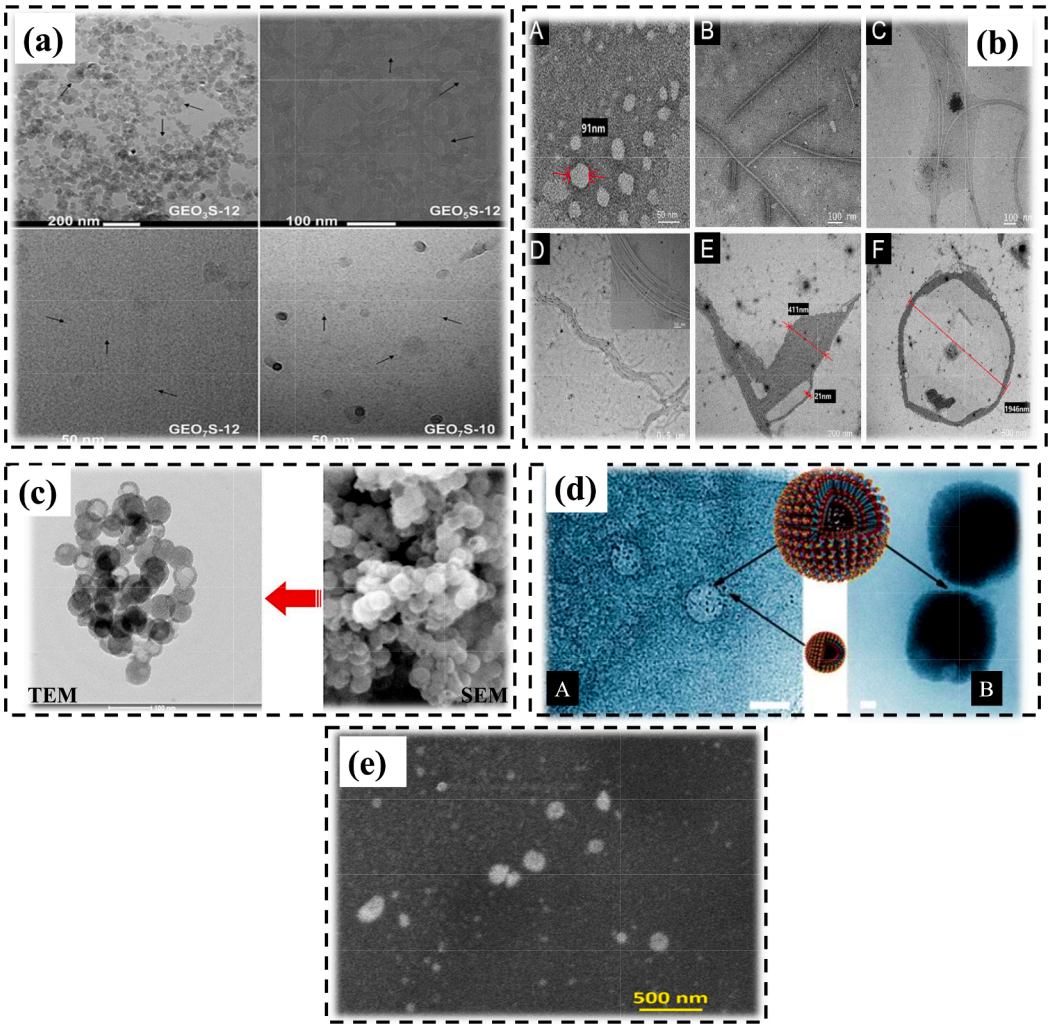

Fig. 8. (a) SEM images of anionic-nonionic Gemini surfactants (GEO_nS-m) aggregate with their vesicle, spherical and rodlike micelles. Reproduced with permission from [51]. Copyrights©, Elsevier 2024. (b) Obtained TEM images of Gemini surfactants at different concentrations for micelles which are; (A) spherical, (B) single rod-shaped, (C) aggregated rod-shaped, (D) composite rod-shaped structure, (E) multilayer, complex structure and (F) ring-like structure in solution of surfactin [52]. (c) TEM and SEM images of spherical structure of cationic Gemini surfactants synthesized by utilizing aromatic spacers with different chain lengths. Reproduced with permission from [53]. Copyrights©, Elsevier 2018. (d) Morphology of surfactants by; (A) cryo-TEM image of (micelles and vesicles are denoted by black arrows) and (B) area-selected ESI images (TEM) of a dried sample [54]. (e) FE-SEM image of micelles which have reverse morphology of the prepared Gemini surfactant [55].

head groups, length and composition of the spacer. Among the surfactants studied, the nonyl bromide-based surfactant stands out with its notably higher electrical conductivity compared to other surfactants. As its concentration increases, its electrical conductivity follows suit, displaying a consistent trend. This trend is in line with the findings observed by Rauniyar et al. [48] who similarly observed that increasing surfactant concentration led to a rapid rise in electrical conductivity.

3.4. Analysis of aggregates morphology

Fig. 6 shows DLS size distribution for aggregates formed by Gemini surfactants with C_9, C_{12} and C_{14} alkyl chains. Fig. 6**(a)** shows that the aggregate diameter for C_9–C_2–C_9[*iso*-Pr(OH)]$_2$ GS in an aqueous solution remains constant at 8–200 nm, regardless of concentration. In Fig. 6 (b), C_{12}–C_2–C_{12}[*iso*-Pr(OH)]$_2$ Gemini surfactant exhibits aggregate diameters ranging from 50 to 200 nm, with a partial increase when the concentration is tripled. Conversely, Fig. 6(c) reveals that the C_{14}–C_2–C_{14}[*iso*-Pr(OH)]$_2$ Gemini surfactant's aggregate diameter increases with higher concentration, increasing from 80 to 120 nm with a three-fold concentration increase. This highlights the inverse relationship between aggregate diameter and alkyl chain length for Gemini surfactants in low-concentration aqueous solutions. Parikh et al. [35] employed Dynamic Light Scattering (DLS) to reveal that the size of the micelles is notably influenced by the nature of the spacer, enhancing our understanding of surfactant behaviour.

3.5. Antimicrobial and antifungal analysis

In Fig. 7, the findings depict the antimicrobial properties displayed by the synthesized Gemini surfactants and their correlation with varying concentrations. Notably, heightened sensitivity against gram-positive bacteria is observed. C_9–C_2–C_9[*iso*-Pr(OH)]$_2$ and C_{14}–C_2–C_{14}[*iso*-Pr(OH)]$_2$ exhibited effective antibacterial characteristics against *S. aureus*, while $C_{14}C_2C_{14}$ [*iso*-Pr(OH)]$_2$ and $C_9C_2C_9$[*iso*-Pr(OH)]$_2$ demonstrate their antimicrobial properties best against *E. coli* and *Candida albicans*, respectively (Fig. 7). However, from C_9 to C_{12}, there is a partial decline in antimicrobial activity, possibly due to surfactant diffusion in the environment. The antibacterial efficacy of GCS escalates with increasing concentration, potentially impacting bacterial membranes via positively charged hydrophilic groups (Fig. 7). The penetration of molecules into the membranes of bacterial and fungal cells is facilitated by the composition of negatively charged microbial cell walls as mentioned

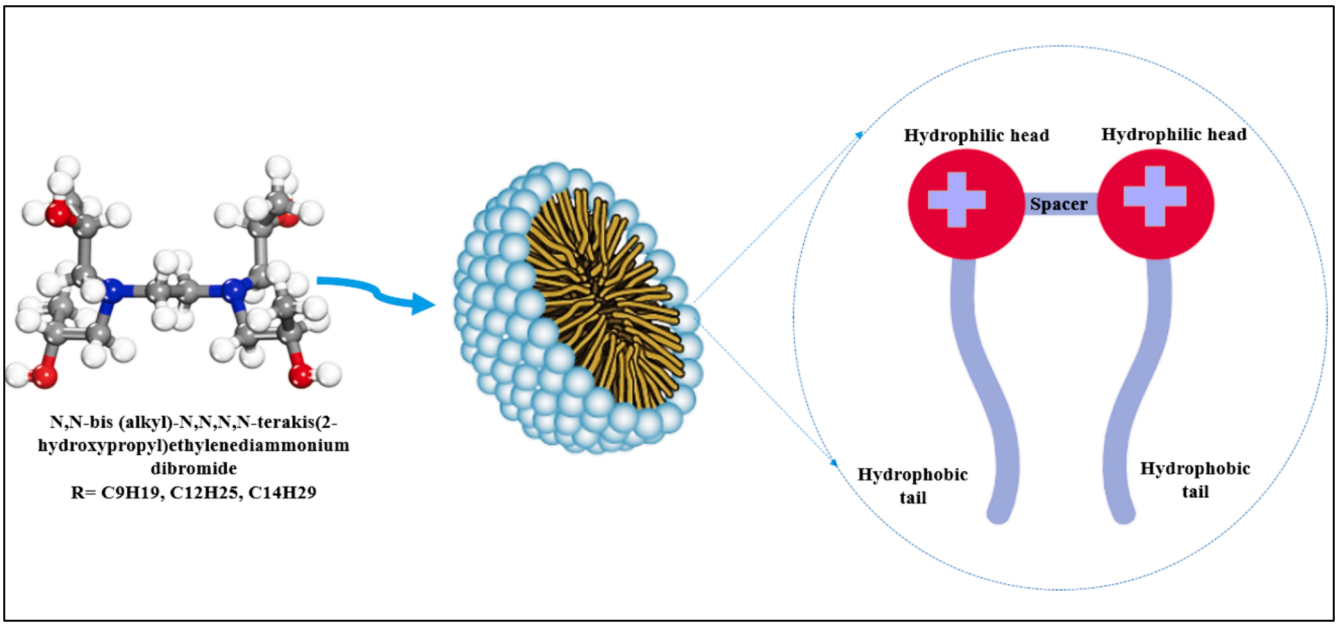

Fig. 9. Overview of the formation of the spherical micelles when a surfactant aggregates in an aqueous medium.

previously in the study of Hao et al. [36]. This penetration process involves a combination of electrostatic and hydrophobic interactions. As discovered by Bao et al. [49], the penetration of GCS molecule into the membrane of the cell is correlated with the length of the alkyl chain. This association highlights the dependence of antimicrobial efficiency on the length of the alkyl chain. Through current extensive research endeavours, a clear trend emerged, indicating that surfactants possessing a C_9 alkyl chain length exhibited a more prominent overall effect. In contrast, the study conducted by Pisarčik et al. [50] gave a different perspective, suggesting that surfactants with a C_{12} alkyl chain length displayed increased efficacy against both bacteria types.

3.6. Exploring micellization

The micellization process orchestrates the assembly of surfactant molecules within a solution, giving rise to diverse structures such as spherical, cylindrical, or double micelles. In the study of Liang et al. [51] was found that with the increase in ethylene oxide content (EO) number of synthesized anionic-nonionic Gemini surfactants (GEO_nS-m) aggregate showed micelles which were vesicle, spherical and rodlike shapes as given in Fig. 8(a). Jiang et al. [52] investigated the morphological characteristics and structural formation of micelles under varying concentrations of surfactant solutions, utilizing negative staining techniques. Through transmission electron microscopy (TEM), they elucidated the micellar structures. Their study revealed that surfactants form spherical micelles only at low concentrations, with a noted decrease in micelle size as the concentration increased. The researchers prepared surfactant solutions at concentrations of 27.6, 18.9, 6.6 and 2.9 g/L to observe these phenomena. Upon examining the micellar structures in fermentation solutions, they monitored any structural changes.

Fig. 8b(A) depicts spherical micelles, while Fig. 8b(B) shows the micellar configuration at a concentration of 2.9 g/L, where rod-shaped micelles were identified. In Fig. 8b(C-D), composite rod-shaped micelles were observed in the solution at 6.6 g/L. As the concentration increased to 18.9 g/L, the rod-shaped micelles began to coalesce, forming more defined structures, as given in Fig. 8b(E). Finally, at the highest concentration of 27.6 g/L, the formation of spherical micelles was observed, as shown in Fig. 8b(F). Similar results were obtained in the study of El-Said et al. [53] as shown in Fig. 8(c). In the study of Bitter et al. [54] was identified the presence of large spherical aggregates alongside smaller micelles in synthesized surfactant solutions, utilizing cryo-transmission electron microscopy (cryo-TEM), as illustrated in Fig. 8(e). Furthermore, Aggrawal et al. [55] employed field emission scanning electron microscopy (FE-SEM) to investigate 12-8-12 reverse micelles. Their analysis revealed micelles with a spherical structure, as given in Fig. 8(f). The predominance of spherical micelle formation is intricately tied to a Critical Packing Parameter (P) of the twin set of active substance molecules, ensuring P is less than or equal to 1/3 ($P \leq 1/3$).

Within these spherical micelles, hydrophilic groups actively participate in electrical and hydrogen bonds, while London forces intricately bind the hydrophobic groups. A critical contributing factor in this dynamic process is the unique molecular structure of Gemini cationic surfactants, featuring two hydrophilic heads and hydrophobic tails within a single molecule. This distinctive configuration plays a pivotal role in spontaneous self-assembly, resulting in enhanced surface activity and performance. The culmination of these interactions manifests as the formation of spherical micelles when a surfactant aggregates in an aqueous medium, as depicted in Fig. 9. Changes in physicochemical properties at various surfactant concentrations, both pre-and post-micellization, provide valuable indicators for assessing micellization parameters. The assessment of CMC for the synthesized cationic Gemini surfactants showing the relationship between concentration (mol/L) and specific conductivity values (μS/cm) is given in Fig. 4.

It exhibits a linear increase in conductivity within both the pre-micellar and micellar concentration ranges of the surfactant, with distinct slopes observed in each of these regions [56]. This underscores the significant impact of the molecular structure of Gemini surfactants on the determination of CMC values [57]. The counterion dissociation degree (α) is evaluated by comparing the slopes observed in the linear segments before and after the breakpoint at CMC. The counterion binding degree (β), representing the number of counterions in the Stern layer that counterbalances the electrostatic force resisting the formation of micelles and counterion dissociation, is calculated using the formula: $\beta = 1 - \alpha$. Table 2 reveals that β values rise as the alkyl chain length decreases. This behaviour is related to the heightened density of surface charge of the micelles, indicating a departure from the results reported by Jia et al. [58].

4. Conclusion

A novel series of cationic Gemini surfactants (Cn-C_2-Cn[*iso*-Pr(OH)]$_2$, n = 9, 12 and 14) were successfully synthesized, followed by a comprehensive evaluation of their performance in the aqueous environment. FTIR spectra confirmed the presence of vital functional groups, O—H group peak at 3378 cm^{-1} and C—N^+ bond stretching at 1088 cm^{-1}. ^{1}H NMR spectra revealed distinct peaks corresponding to various molecular segments, enriching the understanding of GS chemical compositions. The investigation focused on aqueous interfacial activities, aggregation behaviour and antimicrobial efficacy. Remarkably, antimicrobial tests against bacteria and fungi, *Staphylococcus aureus* and *Candida albicans*, unveiled the significant antimicrobial potential of C_{12}–C_2–C_{12} GS at a concentration of 8 mg/L. This finding underscores the potential for tailored surfactant design to combat microbial pathogens effectively. This study showcased the substantial impact of the hydrophobic chain length on the physicochemical characteristics of GS. Surface tension and electrical conductivity measurements at 298 K highlighted these effects, revealing distinct CMC values for different surfactants. Specifically, the CMC value for $C_9C_2C_9$[Iso-Pr(OH)]$_2$ was 0.31, while $C_{14}C_2C_{14}$[Iso-Pr(OH)]$_2$ had a CMC value of 0.48. These surfactants demonstrated varying packing properties, with C_{12}–C_2–C_{12} having a packing value of 1.203 nm, C_9–C_2–C_9 1.504 nm and C_{14}–C_2–C_{14} 0.877 nm, reflecting the customized nature of their packing in the aqueous environment. Insights into aggregate sizes provided by DLS measurements further emphasized the role of alkyl chain length, with C_{14}-based surfactants displaying smaller aggregate sizes compared to others. This research highlights the suitability of the methodologies employed while emphasizing the antimicrobial potential of specific GS. Despite acknowledging its limitations, this research provides valuable information in this field and paves the way for further research, including a broader spectrum of microorganisms and analysis, such as TEM analysis. Future work in this area may lead to advancements in the development of antimicrobial agents, addressing critical challenges in various applications.

CRediT authorship contribution statement

Seyid Zeynab Hashimzada: Writing – review & editing, Validation, Methodology, Investigation, Data curation. **Vagif Abbasov:** Writing – review & editing, Validation, Supervision, Data curation. **Rayen Ben Aoun:** Writing – original draft, Software, Investigation, Formal analysis. **Narcisa Smječanin:** Writing – review & editing, Supervision, Software, Data curation. **Saida Ahmadbayova:** Writing – review & editing, Validation, Supervision, Resources, Funding acquisition, Conceptualization. **Sabah Ansar:** Writing – review & editing. **Farooq Sher:** Project administration, Funding acquisition, Writing – review & editing.

Declaration of competing interest

The authors declare that they have no known competing financial interests or personal relationships that could have appeared to influence the work reported in this paper.

Data availability

Data will be made available on request.

Acknowledgement

This work is also supported by the Institute of Petrochemical Processes of the Ministry of Science and Education of the Republic of Azerbaijan. The authors thank the Researchers Supporting Project number (RSP2024R169), King Saud University, Riyadh, Saudi Arabia for the financial support. The authors are also grateful for the financial support from the International Society of Engineering Science and Technology (ISEST) UK.

References

[1] W.H. Foo, S.S.N. Koay, S.R. Chia, W.Y. Chia, D.Y.Y. Tang, S. Nomanbhay, K. W. Chew, Recent advances in the conversion of waste cooking oil into value-added products: a review, Fuel. 324 (2022) 124539.
[2] J.T. Petkov, J. Penfold, R.K. Thomas, Surfactant self-assembly structures and multilayer formation at the solid-solution interface induces by electrolyte, polymers and proteins, Curr. Opin. Colloid Interface Sci. 57 (2022) 101541.
[3] N. Pal, H. Hoteit, A. Mandal, Structural aspects, mechanisms and emerging prospects of Gemini surfactant-based alternative Enhanced Oil Recovery technology: a review, J. Mol. Liq. 339 (2021) 116811.
[4] P. Bhardwaj, M. Kamil, M. Panda, Surfactant-polymer interaction: effect of hydroxypropylmethyl cellulose on the surface and solution properties of gemini surfactants, Colloid Polym. Sci. 296 (2018) 1879–1889.
[5] Y. Liang, H. Li, M. Li, X. Mao, Y. Li, Z. Wang, L. Xue, X. Chen, X. Hao, Synthesis and physicochemical properties of ester-bonded gemini pyrrolidinium surfactants and a comparison with single-tailed amphiphiles, J. Mol. Liq. 280 (2019) 319–326.
[6] S.S. Moosavi, A.R. Zolghadr, Effect of quaternary ammonium surfactants on biomembranes using molecular dynamics simulation, RSC Adv. 13 (2023) 33175–33186.
[7] C. Zhou, Y. Wang, Structure–activity relationship of cationic surfactants as antimicrobial agents, Curr. Opin. Colloid Interface Sci. 45 (2020) 28–43.
[8] A.R. Ahmady, P. Hosseinzadeh, A. Solouk, S. Akbari, A.M. Szulc, B.E. Brycki, Cationic gemini surfactant properties, its potential as a promising bioapplication candidate, and strategies for improving its biocompatibility: a review, Adv. Colloid Interface Sci. 299 (2022) 102581.
[9] C. Dai, S. Fang, M. Hu, X. He, M. Zhao, X. Wu, S. Yang, Y. Wu, Synthesis, surface adsorption and micelle formation of a class of morpholinium gemini surfactants, J. Ind. Eng. Chem. 54 (2017) 226–233.
[10] Z. Wang, P. Li, K. Ma, Y. Chen, J. Penfold, R.K. Thomas, D.W. Roberts, H. Xu, J. T. Petkov, Z. Yan, The structure of alkyl ester sulfonate surfactant micelles: the impact of different valence electrolytes and surfactant structure on micelle growth, J. Colloid Interface Sci. 557 (2019) 124–134.
[11] J. Wu, H. Gao, D. Shi, Y. Yang, Y. Zhang, W. Zhu, Cationic gemini surfactants containing both amide and ester groups: synthesis, surface properties and antibacterial activity, J. Mol. Liq. 299 (2020) 112248.
[12] M. Wojcieszak, A. Lewandowska, A. Marcinkowska, Ł. Pałkowski, M. Karolak, A. Skrzypczak, A. Syguda, K. Materna, Evaluation of antimicrobial properties of monocationic and dicationic surface-active ionic liquids, J. Mol. Liq. 374 (2023) 121300.
[13] S.M. Shaban, R.M. El-Sherif, M.A. Fahim, Studying the surface behavior of some prepared free hydroxyl cationic amphipathic compounds in aqueous solution and their biological activity, J. Mol. Liq. 252 (2018) 40–51.
[14] H. Shayesteh, F. Raji, A.R. Kelishami, Influence of the alkyl chain length of surfactant on adsorption process: a case study, Surf. Interf. 22 (2021) 100806.
[15] D. Xu, X. Ni, C. Zhang, J. Mao, C. Song, Synthesis and properties of biodegradable cationic gemini surfactants with diester and flexible spacers, J. Mol. Liq. 240 (2017) 542–548.
[16] S.M.S. Hussain, M.S. Kamal, B. El Ali, A.S. Sultan, Synthesis and evaluation of novel Amido-amine cationic Gemini surfactants containing flexible and rigid spacers, J. Surfactants Deterg. 20 (2017) 777–788.
[17] D. Fu, X. Gao, J. Wang, Y. Xie, F. Yang, X. Sui, P. Li, B. Huang, X. Zhang, K. Kan, Micellization, surface activities and thermodynamics study of dialkylpyridinium [C16pymC n][Br](n= 1–4) in aqueous solutions, J. Dispers. Sci. Technol. 42 (2021) 791–801.
[18] M.T. Garcia, O. Kaczerewska, I. Ribosa, B. Brycki, P. Materna, M. Drgas, Hydrophilicity and flexibility of the spacer as critical parameters on the aggregation behavior of long alkyl chain cationic Gemini surfactants in aqueous solution, J. Mol. Liq. 230 (2017) 453–460.
[19] T.F. Moghadam, S. Azizian, S. Wettig, Effect of spacer length on the interfacial behavior of N,N′-bis (dimethylalkyl)-α, ω-alkanediammonium dibromide gemini surfactants in the absence and presence of ZnO nanoparticles, J. Colloid Interface Sci. 486 (2017) 204–210.
[20] K. Taleb, M. Mohamed-Benkada, N. Benhamed, S. Saidi-Besbes, Y. Grohens, A. Derdour, Benzene ring containing cationic gemini surfactants: synthesis, surface properties and antibacterial activity, J. Mol. Liq. 241 (2017) 81–90.
[21] S.M.S. Hussain, M.S. Kamal, M. Murtaza, Synthesis of novel ethoxylated quaternary ammonium gemini surfactants for enhanced oil recovery application, Energies. 12 (2019) 1731.
[22] Z. Huang, J. Mao, M. Cun, X. Yang, C. Lin, Y. Zhang, H. Zhang, J. Mao, Q. Wang, Q. Zhang, Polyhydroxy cationic viscoelastic surfactant for clean fracturing fluids: study on the salt tolerance and the effect of salt on the high temperature stability of wormlike micelles, J. Mol. Liq. 366 (2022) 120354.
[23] Q.-X. Mei, L. Lai, S.-J. Li, P. Mei, Y.-Q. Wang, Q.-L. Ma, Y. Liu, Surface properties and phase behavior of Gemini/conventional surfactant mixtures based on multiple quaternary ammonium salts, J. Mol. Liq. 281 (2019) 506–516.
[24] B. Shojaei, M. Abtahi, M. Najafi, Chemical recycling of PET: a stepping-stone toward sustainability, Polym. Adv. Technol. 31 (2020) 2912–2938.
[25] H. Kumar, J. Kaur, P. Awasthi, Scrutinizing the micellization behaviour of 14-2-14 gemini surfactant and tetradecyltrimethylammonium bromide in aqueous solutions of betaine hydrochloride drug, J. Mol. Liq. 338 (2021) 116642.
[26] O. Kaczerewska, B. Brycki, I. Ribosa, F. Comelles, M.T. Garcia, Cationic gemini surfactants containing an O-substituted spacer and hydroxyethyl moiety in the

polar heads: self-assembly, biodegradability and aquatic toxicity, J. Ind. Eng. Chem. 59 (2018) 141–148.
[27] S.M.S. Hussain, M.S. Kamal, T. Solling, M. Murtaza, L.T. Fogang, Surface and thermal properties of synthesized cationic poly (ethylene oxide) gemini surfactants: the role of the spacer, RSC Adv. 9 (2019) 30154–30163.
[28] M. Pisárčik, M. Polakovičová, M. Markuliak, M. Lukáč, F. Devínsky, Self-assembly properties of cationic gemini surfactants with biodegradable groups in the spacer, Molecules. 24 (2019) 1481.
[29] Z. Wang, H. Song, The synthesis of quaternary N-alkyl tropinium cationic surfactants and study on their properties: effect of temperature, hydrophobic chain length and anions, J. Mol. Struct. 1268 (2022) 133732.
[30] T. Sugahara, Y. Takamatsu, A. Bhadani, M. Akamatsu, K. Sakai, M. Abe, H. Sakai, Characterization of the micelle structure of oleic acid-based gemini surfactants: effect of stereochemistry, Phys. Chem. Chem. Phys. 20 (2018) 8874–8880.
[31] R.L. Anderson, D.J. Bray, A. Del Regno, M.A. Seaton, A.S. Ferrante, P.B. Warren, Micelle formation in alkyl sulfate surfactants using dissipative particle dynamics, J. Chem. Theory Comput. 14 (2018) 2633–2643.
[32] M. Akram, H. Lal, M. Osama, F. Ansari, S. Anwar, A. Ahmad, N. Samreen, H. M. Azum, A.M.A. Marwani, An insight view on synthetic protocol, surface activity, and biological aspects of novel biocompatible quaternary ammonium cationic gemini surfactants, J. Surfact. Deterg. 24 (2021) 35–49.
[33] L. Vasileva, G. Gaynanova, F. Valeeva, E. Romanova, R. Pavlov, D. Kuznetsov, G. Belyaev, I. Zueva, A. Lyubina, A. Voloshina, Synthesis, properties, and biomedical application of dicationic gemini surfactants with dodecane spacer and carbamate fragments, Int. J. Mol. Sci. 24 (2023) 12312.
[34] N.R. Indla, Y. Maruthi, R. Rawat, T.S. Kumar, N.R. Reddy, M. Sharma, T. M. Aminabhavi, R.R. Kakarla, A.V.S. Sainath, Synthesis and biological properties of novel glucose-based fluoro segmented macromolecular architectures, Int. J. Biol. Macromol. 268 (2024) 131724.
[35] K. Parikh, S. Singh, A. Desai, S. Kumar, An interplay between spacer nature and alkyl chain length on aqueous micellar properties of cationic Gemini surfactants: a multi-technique approach, J. Mol. Liq. 278 (2019) 290–298.
[36] J. Hao, T. Qin, Y. Zhang, Y. Li, Y. Zhang, Synthesis, surface properties and antimicrobial performance of novel gemini pyridinium surfactants, Colloids Surf. B Biointerf. 181 (2019) 814–821.
[37] M.A. Betiha, S.B. El-Henawy, A.M. Al-Sabagh, N.A. Negm, T. Mahmoud, Experimental evaluation of cationic-Schiff base surfactants based on 5-chloro-methyl salicylaldehyde for improving crude oil recovery and bactericide, J. Mol. Liq. 316 (2020) 113862.
[38] P. Wang, H. Han, C. Tian, R. Liu, Y. Jiang, Experimental study on dust reduction via spraying using surfactant solution, Atmos. Pollut. Res. 11 (2020) 32–42.
[39] İ. Sarıkaya, S. Bilgen, H. Akbaş, Investigation of mixing behavior of both a conventional surfactant and different inorganic salts with a cationic gemini surfactant in aqueous solution, J. Surfact. Deterg. 22 (2019) 1319–1330.
[40] C. Ren, F. Wang, Z. Zhang, H. Nie, N. Li, M. Cui, Synthesis, surface activity and aggregation behavior of Gemini imidazolium surfactants 1, 3-bis (3-alkylimidazolium-1-yl) propane bromide, Colloids Surf. A Physicochem. Eng. Asp. 467 (2015) 1–8.
[41] M.H. Alimohammadi, S. Javadian, H. Gharibi, A. Reza Tehrani-Bagha, M. R. Alavijeh, K. Kakaei, Aggregation behavior and intermicellar interactions of cationic Gemini surfactants: effects of alkyl chain, spacer lengths and temperature, J. Chem. Thermodyn. 44 (2012) 107–115.
[42] A. Shaheen, R. Arif, Synthesis, micellization behaviour and cytotoxic properties of imidazolium-based Gemini surfactants, Colloid Interface Sci. Commun. 36 (2020) 100257.
[43] D. Kumar, N. Azum, M.A. Rub, A.M. Asiri, Aggregation behavior of sodium salt of ibuprofen with conventional and Gemini surfactant, J. Mol. Liq. 262 (2018) 86–96.
[44] S. Singh, K. Parikh, S. Kumar, V.K. Aswal, S. Kumar, Spacer nature and composition as key factors for structural tailoring of anionic/cationic mixed gemini micelles: Interaction and solubilization studies, J. Mol. Liq. 279 (2019) 108–119.
[45] T. Zhao, N. Feng, Y. Zhao, C. Gong, Adsorption properties and aggregation behavior of mixed system of anionic/cation surfactants with different structures, J. Mol. Liq. 337 (2021) 116341.
[46] T. Sahara, D. Wongsawaeng, K. Ngaosuwan, W. Kiatkittipong, P. Hosemann, S. Assabumrungrat, Highly effective removal of perfluorooctanoic acid (PFOA) in water with DBD-plasma-enhanced rice husks, Sci. Rep. 13 (2023) 13210.
[47] A. Żak, G. Łazarski, M. Wytrwal-Sarna, D. Jamróz, M. Górniewicz, A. Foryś, B. Trzebicka, M. Kepczynski, Molecular insights into the self-assembly of hydrophobically modified chondroitin sulfate in aqueous media, Carbohydr. Polym. 297 (2022) 119999.
[48] H. Zhu, Z. Hu, X. Ma, J. Wang, D. Cao, Synthesis, surface and antimicrobial activities of cationic Gemini surfactants with semi-rigid spacers, J. Surfact. Deterg. 19 (2016) 265–274.
[49] Y. Bao, Y. Zhang, J. Guo, J. Ma, Y. Lu, Application of green cationic silicon-based Gemini surfactants to improve antifungal properties, fiber dispersion and dye absorption of sheepskin, J. Clean. Prod. 206 (2019) 430–437.
[50] M. Pisárčik, M. Bajcura, M. Lukáč, F. Devínsky, A. Bilková, F. Bilka, B. Horváth, Self-aggregation of cationic Gemini surfactants with amide groups in the spacer and variable alkyl chain length, Colloid Polym. Sci. 301 (2023) 1379–1392.
[51] X. Liang, J. Dong, W. Zhang, Y. Mo, Y. Li, J. Bai, Solubilization mechanism and mass-transfer model of anionic-nonionic Gemini surfactants for chlorinated hydrocarbons, Sep. Purif. Technol. 330 (2024) 125534.
[52] R. Jiang, L. Cai, M. Wang, H. Yu, Micelle morphology observation method of lipopeptide by negative-staining-based transmission electron microscopy, Biotechnol. Notes. 3 (2022) 75–78.
[53] W.A. El-Said, A.S. Moharram, E.M. Hussein, A.M. El-Khawaga, Design, synthesis, anticorrosion efficiency, and applications of novel Gemini surfactants for preparation of small-sized hollow spheres mesoporous silica nanoparticles, Mater. Chem. Phys. 211 (2018) 123–136.
[54] S. Bitter, M. Schlötter, M. Schilling, M. Krumova, S. Polarz, R.F. Winter, Ferro-self-assembly: magnetic and electrochemical adaptation of a multiresponsive zwitterionic metalloamphiphile showing a shape-hysteresis effect, Chem. Sci. 12 (2021) 270–281.
[55] R. Aggrawal, S. Kumari, S. Gangopadhyay, S.K. Saha, Role of different states of solubilized water on solvation dynamics and rotational relaxation of coumarin 490 in reverse micelles of gemini surfactants, water/12-s-12.2 Br–(s= 5, 6, 8)/n-propanol/cyclohexane, ACS Omega. 5 (2020) 6738–6753.
[56] V. Chauhan, M. Kumar, I. Soni, P. Shandilya, S. Singh, Synthesis, physical properties and cytotoxic assessment of ester-terminated gemini imidazolium surfactants, J. Mol. Liq. 387 (2023) 122645.
[57] B. Brycki, A. Szulc, J. Brycka, I. Kowalczyk, Properties and applications of quaternary ammonium gemini surfactant 12-6-12: an overview, Molecules. 28 (2023) 6336.
[58] X. Jia, R. Wei, B. Xu, H. Liu, B.-C. Xu, Green synthesis, surface activity, micellar aggregation, and foam properties of amide quaternary ammonium surfactants, ACS Omega. 7 (2022) 48240–48249.
[59] D. Fu, X. Gao, B. Huang, J. Wang, Y. Sun, W. Zhang, K. Kan, X. Zhang, Y. Xie, X. Sui, Micellization, surface activities and thermodynamics study of pyridinium-based ionic liquid surfactants in aqueous solution, RSC Adv. 9 (2019) 28799–28807.
[60] C. Kang, J. Wu, Y. Zheng, L. Lai, Studies on the surface properties and microaggregates of cationic/anionic surfactant mixtures based on sulfonate gemini surfactant, J. Mol. Liq. 320 (2020) 114431.
[61] W. Yang, Y. Cao, H. Ju, Y. Wang, Y. Jiang, T. Geng, Amide Gemini surfactants linked by rigid spacer group 1, 4-dibromo-2-butene: Surface properties, aggregate and application properties, J. Mol. Liq. 326 (2021) 115339.